Table III. Fractional Atomic Coordinates with Estimated Standard Deviations in Parentheses

atom	*x/a*	*y/b*	*z/c*
W	0.28322 (3)	0.56915 (2)	0.25327 (2)
Rh(1)	0.41513 (6)	0.67772 (3)	0.19097 (3)
Rh(2)	0.54838 (6)	0.77899 (3)	0.12970 (3)
P(1)	0.2000 (2)	0.6768 (1)	0.1900 (1)
P(2)	0.5134 (2)	0.5811 (1)	0.2447 (1)
C(1)	0.2614 (8)	0.5165 (4)	0.1564 (4)
O(1)	0.2433 (6)	0.4866 (3)	0.1023 (3)
C(2)	0.3164 (9)	0.4764 (5)	0.3040 (5)
O(2)	0.3335 (8)	0.4241 (4)	0.3333 (4)
C(3)	0.3059 (8)	0.6257 (5)	0.3471 (4)
O(3)	0.3184 (7)	0.6591 (4)	0.3992 (4)
C(4)	0.1017 (8)	0.5610 (4)	0.2753 (4)
O(4)	−0.0019 (6)	0.5579 (4)	0.2897 (4)
C(5)	0.4607 (8)	0.6958 (4)	0.0873 (4)
O(5)	0.4366 (6)	0.6638 (3)	0.0338 (3)
C(6)	0.5026 (8)	0.7619 (4)	0.2322 (4)
O(6)	0.5100 (6)	0.7832 (4)	0.2928 (3)
C(7)	0.5878 (8)	0.8164 (4)	0.0159 (4)
C(8)	0.6864 (7)	0.7750 (5)	0.0419 (4)
C(9)	0.8075 (8)	0.8025 (5)	0.0741 (5)
C(10)	0.7958 (8)	0.8660 (5)	0.1248 (5)
C(11)	0.6809 (8)	0.8626 (4)	0.1710 (4)
C(12)	0.5678 (8)	0.8930 (4)	0.1513 (5)
C(13)	0.5415 (8)	0.9330 (5)	0.0817 (5)
C(14)	0.5889 (9)	0.8966 (4)	0.0129 (5)
C(15)	0.1060 (5)	0.6681 (3)	0.1050 (3)
C(16)	0.0149 (5)	0.6158 (3)	0.0950 (3)
C(17)	−0.0534 (5)	0.6114 (3)	0.0287 (3)
C(18)	−0.0305 (5)	0.6594 (3)	−0.0276 (3)
C(19)	0.0607 (5)	0.7117 (3)	−0.0175 (3)
C(20)	0.1290 (5)	0.7160 (3)	0.0488 (3)
C(21)	0.1153 (4)	0.7385 (3)	0.2471 (3)
C(22)	0.1825 (4)	0.7809 (3)	0.2971 (3)
C(23)	0.1191 (4)	0.8245 (3)	0.3453 (3)
C(24)	−0.0115 (4)	0.8258 (3)	0.3435 (3)
C(25)	−0.0787 (4)	0.7835 (3)	0.2935 (3)
C(26)	−0.0153 (4)	0.7398 (3)	0.2453 (3)
C(27)	0.6115 (4)	0.5279 (3)	0.1855 (2)
C(28)	0.7235 (4)	0.4967 (3)	0.2099 (2)
C(29)	0.7962 (4)	0.4591 (3)	0.1610 (2)
C(30)	0.7569 (4)	0.4527 (3)	0.0876 (2)
C(31)	0.6448 (4)	0.4839 (3)	0.0632 (2)
C(32)	0.5721 (4)	0.5215 (3)	0.1122 (2)
C(33)	0.6081 (5)	0.5923 (3)	0.3296 (3)
C(34)	0.5760 (5)	0.5574 (3)	0.3938 (3)
C(35)	0.6443 (5)	0.5698 (3)	0.4590 (3)
C(36)	0.7447 (5)	0.6170 (3)	0.4599 (3)
C(37)	0.7768 (5)	0.6519 (3)	0.3958 (3)
C(38)	0.7085 (5)	0.6396 (3)	0.3306 (3)

m (8 H) ppm. ^{31}P NMR ($CDCl_3$ solution): 177 dd ppm ($J_1 = 158$ Hz; J_2 4.7 Hz J_{PW} 167.3 Hz).

X-ray Structure Analysis. The experimental parameters are listed in Table II. The crystal was sealed on a glass fiber and transferred to a CAD4 Enraf-Nonius diffractometer automated with a Microvax 2000 computer.

The unit cell was refined by using 25 reflections in the 2θ range of 22–26°. A total of 6822 intensity data, up to $2\theta = 50°$, were collected in the $\theta/2\theta$ scan mode (scan width 0.80° + 0.35° tan θ, scan speed 1.1–8.4° min^{-1}). A set of three standard reflections was measured every 2 h of exposure time, with no noticeable change in intensity observed during the collection. Lorentz–polarization and empirical absorption[12] corrections were made with SDP.[13]

The structure was solved by a Patterson map calculation, and the refinement and difference-Fourier processes were completed with SHELX 76[14] using 4279 reflections having $I > 3\sigma(I)$ out of the 6462 independent ones. The atomic scattering factors are those of ref 15 for heavy atoms and those of ref 16 for hydrogens. Full-matrix least-squares techniques were used with phenyl rings refined as isotropic rigid groups (C–C = 1.395 Å). All H atoms were observed but introduced in calculations in constrained geometry (C–H = 0.97 Å) with a temperature factor U = 0.07 Å^2, kept fixed. All other atoms were refined anisotropically. The refinement converged with a maximum shift/esd of 0.006 on the final cycle with 274 variable parameters. A good fit of S = 1.35 for the data using the weighting scheme $w = [\sigma^2(F_o) + 0.0002F_o^2]^{-1}$ was obtained. The maximum residual peak was near the W atom at 0.82 e Å^{-3}. Fractional atomic coordinates are given in Table III.

Supplementary Material Available: For **2**, tables of hydrogen atom coordinates, anisotropic thermal parameters, all bond distances and bond angles, and least-squares plane equations (5 pages); a table of calculated and observed structure factors (6 pages). Ordering information is given on any current masthead page.

---

(12) North, A. C. T.; Phillips, D. C.; Matthews, F. S. *Acta Crystallogr., Sect. A* **1968**, *A24*, 351.

(13) Frentz, B. A. *SDP Structure Determination Package*; Enraf-Nonius: Delft, Holland, 1982.

(14) Sheldrick, G. M. "SHELX76. Program for Crystal Structure Determination"; University of Cambridge, Cambridge, U.K., 1976.

(15) *International Tables for X-ray Crystallography*; Kynoch Press: Birmingham, U.K., 1974; Vol. IV.

(16) Stewart, R. F.; Davidson, E. R.; Simpson, W. T. *J. Chem. Phys.* **1965**, *42*, 3175.

Contribution from the Department of Chemistry, BG-10,
University of Washington, Seattle, Washington 98195

Photochemical Reactions of the Binuclear Platinum(II) Diphosphite Complex $Pt_2(P_2O_5H_2)_4^{4-}$ with Disubstituted Silanes

Y. Huang and B. E. Eichinger*

Received February 8, 1989

The photochemical properties of the intensity luminescent, binuclear platinum(II) diphosphite complex $Pt_2(P_2O_5H_2)_4^{4-}$ (Pt_2) have attracted much interest in recent years.[1-10] The long microsecond lifetime (τ = 9.8 μs) of $^3Pt_2^*$ makes it feasible to carry out chemical reactions with this triplet excited state.[3-9] It was reported that the triplet excited state $^3Pt_2^*$ has a unique reactivity to transfer hydrogen atoms from several organic substrates with relatively weak C–H bonds.[8-10] Hydrogen atom transfer, $RH + {}^3Pt_2^* \rightarrow R^{\bullet} + Pt_2H$ was proposed by Roundhill to be the primary photoprocess in the photoinduced reactions of $^3Pt_2^*$ with RH. Gray et al.[11-13] recently reported the results of hydrogen atom transfer from triaryl- or trialkyl-substituted organometallic hydrides of Sn, Ge, and Si by $^3Pt_2^*$ and thereby provided support for Roundhill's proposal.

In order to explore the reactions of $^3Pt_2^*$ with bonds other than C–H for their potential applications, the photochemical reactions of Pt_2 with disubstituted silanes $R^1R^2SiH_2$ have been preliminarily examined. This work provides further support for the hydrogen

---

(1) Che, C.-M.; Butler, L. G.; Grunthaner, P. J.; Gray, H. B. *Inorg. Chem.* **1985**, *24*, 4662.

(2) Rice, S. F.; Gray, H. B. *J. Am. Chem. Soc.* **1983**, *105*, 4571.

(3) Che, C.-M.; Cho, K.-C.; Chan, W.-S.; Gray, H. B. *Inorg. Chem.* **1986**, *25*, 4906.

(4) Che, C.-M.; Butler, L. G.; Gray, H. B. *J. Am. Chem. Soc.* **1981**, *103*, 7796.

(5) Milder, S. J.; Goldbeck, R. A.; Kliger, D. S.; Gray, H. B. *J. Am. Chem. Soc.* **1980**, *102*, 6761.

(6) Che, C.-M.; Schaefer, W. P.; Gray, H. B.; Dickson, M. K.; Stein, P. B.; Roundhill, D. M. *J. Am. Chem. Soc.* **1982**, *104*, 4253.

(7) Marshall, J. L.; Stobart, S. R.; Gray, H. B. *J. Am. Chem. Soc.* **1984**, *106*, 3027.

(8) Marshall, J. L.; Stiegman, A. E.; Gray, H. B. In *Excited States and Reactive Intermediates*; Lever, A. B. P., Ed.; ACS Symposium Series 307, American Chemical Society: Washington, DC, 1986; pp 166–176.

(9) Roundhill, D. M. *J. Am. Chem. Soc.* **1985**, *107*, 4354.

(10) Roundhill, D. M.; Atherton, S. J.; Shen, Z.-P. *J. Am. Chem. Soc.* **1987**, *109*, 6077.

(11) Vlcek, Antonin, Jr.; Gray, H. B. *J. Am. Chem. Soc.* **1987**, *109*, 286.

(12) Vlcek, Antonin, Jr.; Gray, H. B. *Inorg. Chem.* **1987**, *26*, 1997.

(13) Harvey, E. L.; Stiegman, A. E.; Vlcek, Antonin, Jr.; Gray, H. B. *J. Am. Chem. Soc.* **1987**, *109*, 5233.

0020-1669/90/1329-0565$02.50/0

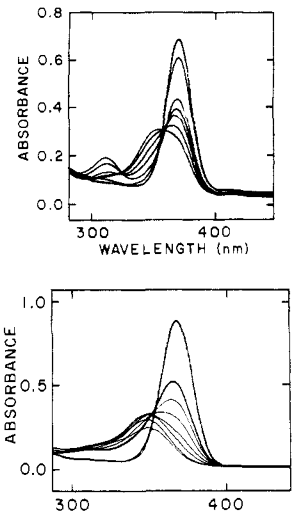

Figure 1. UV absorption spectra changes for reactions of Pt_2 with $R^1R^2SiH_2$ in CH_3CN under argon on irradiation at 366 nm. (a) Ph_2SiH_2. Irradiation time from the top to the bottom of the absorbance at 370 nm (min): 0, 3, 5, 7, 9, 12, 15. (b) $MePhSiH_2$. Irradiation time from the top to the bottom of the absorbance at 370 nm (min): 0, 5, 7, 9, 12, 15, 30, 60.

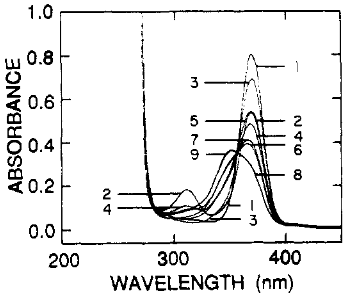

Figure 2. Changes in the UV absorption spectra during the course of the reaction of Pt_2 with Ph_2SiH_2 under argon with alternating irradiation of 366 and >300 nm. Curve 1: initial, no irradiation. Curve 2: 3 min at 366 nm. Curve 3: after additional 1 min irradiation with $\lambda > 300$ nm. Curves 4–9: repeat sequence as for curves 2 and 3, i.e., an additional 3 min at 366 nm, then another 1 min with >300 nm, etc.

atom transfer reactions of $^3Pt_2{}^*$.

Results and Discussion

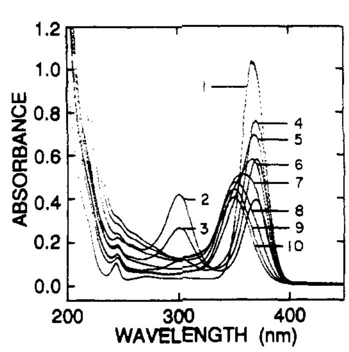

Figure 3. Changes in the UV absorption spectra during the course of reactions of Pt_2 with Et_2SiH_2 in CH_3CN under argon with 366-nm radiation. Irradiation time of curves 1–10 (min): 0, 1, 2, 3, 5, 7, 12, 30, 60, 120.

Reactions of Pt_2 with Diphenylsilane and Methylphenylsilane on Irradiation (λ = 366 nm). The changes of the ultraviolet absorption spectra during the course of the reaction of Pt_2 with an excess of Ph_2SiH_2 or $MePhSiH_2$ in CH_3CN under argon are shown in Figure 1. In the initial period of irradiation, a new absorbance at 313 nm increases rapidly to a maximum value and an absorption at 350 nm rises gradually as the intensity of the absorbance at 370 nm decreases. It was reported[8,11-13] that the hydrogen atom abstraction by $^3Pt_2{}^*$ from R_3EH (E = Sn, Ge, Si) or organic species with weak C–H bonds formed a reaction product, platinum dihydride, which had a UV absorbance at 314 nm. This species could change back to Pt_2 under 313-nm radiation or broad-band UV irradiation. This was verified by work in our laboratory (Figure 2). As can be seen, 3 min of 366-nm radiation caused a remarkable reduction in the intensity of the absorbance at 370 nm and the appearance of the absorbance at 313 nm. Subsequent irradiation with $\lambda > 300$ nm for 1 min resulted in the disappearance of the peak at 313 nm and a concomitant enhancement in the absorbance at 370 nm. About 86% of the original Pt_2 was recovered by this photochemical back-reaction. Repetition of this alternating irradiation gave rise to the reappearance of these phenomena, although the relative amount of Pt_2 recovered depends on the time of the previous photolysis. When the irradiation was interrupted, Pt_2H_2 was converted back to Pt_2 quickly even on standing in the dark at ambient conditions. The extent to which $^3Pt_2{}^*$ reacts with silanes to form Pt_2H_2 and the stability of Pt_2H_2 produced are dependent on the nature of the silanes. Therefore, there is no doubt about the occurrence both of hydrogen atom abstraction by $^3Pt_2{}^*$ from disubstituted silanes bearing at least one aryl group bound to the silicon atom and of the product platinum dihydride. It is obvious that the following mechanism proposed by Roundhill[10] for the photochemical reactions between Pt_2 and RH should apply to the photochemical reactions of Pt_2 with $R^1R^2SiH_2$:

$$Pt_2 \xrightarrow{h\nu} {}^3Pt_2{}^* \tag{1}$$

$$^3Pt_2{}^* + R^1R^2SiH_2 \rightarrow Pt_2H + HR^1R^2Si^\bullet \tag{2}$$

$$2Pt_2H \rightarrow Pt_2H_2 + Pt_2 \tag{3}$$

$$Pt_2H_2 \xrightarrow[\text{(or on standing)}]{h\nu\ (>300\ \text{nm})} Pt_2 + H_2 \tag{4}$$

However, as shown in Figure 1, complete conversion of Pt_2 to Pt_2H_2 was not achieved. As irradiation continued, the intensity of the absorbance at 313 nm diminished, the absorbance at 370 nm continued to diminish, and the intensity of the absorbance at 350 nm increased noticeably. The absorbances at 313 and 370 nm disappeared at last, and there was only the absorbance at 350 nm remaining. These changes show that the product Pt_2H_2 undergoes secondary photochemical reactions on irradiation at 366 nm. It appears that Pt_2H_2 reacts with the silanes as well as other unidentified silicon-containing photolytic products.

Reaction of Pt_2 with Diethylsilane on Irradiation (λ = 366 nm). The changes in the ultraviolet absorption spectra during the reactions of $^3Pt_2{}^*$ with an excess of Et_2SiH_2 in CH_3CN under argon are shown in Figure 3. In the initial period or irradiation, a new absorbance at 301 nm appeared and increased sharply to a maximum value as the intensity of the absorbance at 370 nm decreased. Obviously, a product that has an absorbance at 301 nm was formed. However, complete conversion of Pt_2 was also not achieved. As irradiation continued, the intensity of the peak at 301 nm decreased quickly with a concomitant increase of the Pt_2 absorbance at 370 nm. This shows that this product is converted back to Pt_2 on irradiation at 366 nm. Moreover, when the irradiation is interrupted, this product can also change back to Pt_2 quickly on standing even in the dark at ambient temperature. Therefore, it appears to be reasonable to assume that the product which absorbs at 301 nm possesses the structure HPt_2SiEt_2H, which might be formed by in-cage recombination of HPt_2 and $HEt_2Si^\bullet$. It is understandable that this product is quite unstable and tends strongly to reductively eliminate Et_2SiH_2 to regenerate Pt_2. The following mechanism is proposed for the photochemical reactions of Pt_2 with Et_2SiH_2:

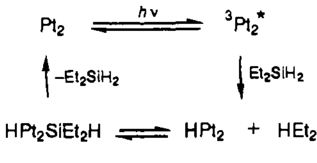

(5)

Evidence for the existence of products $HPt_2SiR^1R^2$ has not been found for the reactions of Pt_2 with Ph_2SiH_2 or $MePhSiH_2$. This might be attributed to the difference in the reactivity of $HR^1R^2Si^{\bullet}$ radicals. The stability of $HR^1R^2Si^{\bullet}$ radicals decreases in a sequence of $HPh_2Si^{\bullet} > HMePhSi^{\bullet} > HEt_2Si^{\bullet}$. Clearly, $HEt_2Si^{\bullet}$ radicals have the largest reactivity toward recombination with HPt_2 in cage.

As can be seen in Figure 3, a gradual rise in the absorption at 350 nm during irradiation reveals the occurrence of secondary photoprocesses. Prolonged irradiation (5 min and longer) causes the disappearance of the absorbance at 301 nm and the shift of the main absorption band from 370 to 350 nm. Owing to high reactivity of $HR^1R^2Si^{\bullet}$ radicals, their reactions with Pt_2 or unreacted $R^1R^2SiH_2$ or solvent or other unidentified silicon-containing photolytic products are probable,[11,14] either singly or collectively.

It appears that the photochemical reactions of Pt_2 with disubstituted silanes in CH_3CN under argon are quite complicated. The proton-coupled ^{31}P NMR spectra of the reaction mixture of Pt_2 and Et_2SiH_2 after photolysis exhibit the chemical shifts $\delta = -10.1, -9.3$, and -8.5 ppm with $J(P-H) = 577$, 573, and 584 Hz, respectively.[15] The magnitudes of these ^{31}P chemical shifts and P–H coupling constants are in accord with the structures of salts or derivatives of phosphorous acid or pyrophosphorous acid in which there are hydrogen atoms attached directly to phosphorus atoms.[16] This signifies that the disassembly of the binuclear platinum diphosphite complexes occurs during photolysis. Attack of $HR^1R^2Si^{\bullet}$ radicals on P–Pt and O–H bonds of $Pt_2(P_2O_5H_2)_4^{4-}$ cannot be excluded.

Experimental Section

Materials. K_2PtCl_4, H_3PO_3, and Bu_4NCl were purchased from Aldrich Chemical Co. Bu_4NCl was purified by recrystallization from benzene and petroleum ether. Deionized water was degassed with argon in advance. Acetonitrile of analytical reagent grade was dried and distilled over P_2O_5 under argon directly prior to use. Disubstituted silanes were dried over 4-Å molecular sieves and distilled under argon (at reduced pressures for Ph_2SiH_2 and $MePhSiH_2$). A UV lamp (UVP Inc., UVGL-25, 4 W) was used as a radiation source of narrow-band light centered on 366 nm. A second UV lamp (UVP Inc., UVS-11) was modified by the replacement of the 254-nm filter with a Pyrex glass filter for use as a radiation source for $\lambda > 300$ nm UV light.

Synthesis of $(Bu_4N)_4Pt_2(P_2O_5H_2)_4$. Gray's method[1] was followed. The purity of Pt_2 was checked by ^{31}P NMR. ^{31}P NMR: δ 68.3, $J(^{31}P-^{195}Pt) = 2975$ Hz. No other peaks were observed in the ^{31}P NMR spectrum. This complex has an extinction coefficient of 3.37×10^4 M^{-1} cm^{-1}.

Reactions of Pt_2 with Disubstituted Silanes under 366-nm Radiation. All the reactions, except those for preparation of samples for measurements of ^{31}P NMR, were carried out in acetonitrile under argon in a 1-cm quartz cell (for UV measurements). Pt_2 was degassed under vacuum and purged with argon prior to use. The concentrations of Pt_2 were $(2.80 \pm 0.80) \times 10^{-5}$ mol/L. The mole ratio of Pt_2 to silane was 1:300 in all experiments. The reaction mixture was irradiated with UV light of $\lambda = 366$ nm at 23 ± 2 °C immediately after preparation. The reaction was followed by UV measurements at different irradiation times.

The samples used for measurements of ^{31}P NMR spectra were prepared by irradiating a reaction mixture in which the concentration of Pt_2 was 3.30×10^{-3} mol/L and the mole ratio of Pt_2 to Et_2SiH_2 was 1:300. The radiation source of 366 nm was a 500-W Hanovia medium-pressure mercury lamp enclosed in a water-cooled Pyrex glass well, combined with an interference filter PSR35-3078 from the Ealing Co. All procedures were carried out under argon. The progress of the reaction was traced by UV measurements for the samples taken at different irradiation times. The UV irradiation was stopped when the position of the absorbance above 300 nm moved to 350 nm. The solvent and unreacted silane were removed under vacuum at room temperature to increase the concentration for ^{31}P NMR measurements.

Instrumentation. Ultraviolet absorption spectra were measured in CH_3CN on a HP-8450 UV/vis spectrophotometer. The 121.4-MHz ^{31}P NMR spectra were obtained on a Varian VXR 300-MHz NMR spectrometer, relative to external 85% H_3PO_4, with CD_3CN used as solvent.

Acknowledgment. This work was supported by grants from the IBM Corp. and the Department of Energy (DE-FG06-84ER45123). Their financial assistance is greatly appreciated.

---

(14) Armitage, D. A.; Riviere, P.; Riviere-Baudet, M.; Satge, J.; Davies, A. G.; Smith, P. J. In *Comprehensive Organometallic Chemistry*, Wilkinson, G., Stone, F. G. A., Abel, E. W., Eds.; Pergamon: Oxford, England, 1982; Vol. 2; pp 91–92, 1–203, 399–627.

(15) There are three other main chemical shifts $\delta = 58.68$, 58.84, and 51.1 ppm with $J(^{195}Pt-^{31}P) = 3096$, 3059, and 3260 Hz and $J(P-H) = 6.4$, 5.5, and 0 Hz, respectively. The structures of the compounds that these ^{31}P chemical shifts and coupling constants represent are not yet clear. Attack of HR^1R^2Si radicals on the P–O bonds of $P_2O_5H_2^{2-}$ cannot be excluded.

(16) Crutchfield, M. M.; Dungan, C. H.; Letcher, J. H.; Mark, V.; Van Wazer, J. R. *^{31}P Nuclear Magnetic Resonance*; Topics in Phosphorus Chemistry 5; Interscience: New York, 1967; pp 47, 290–291.

Contribution from the Department of Chemistry,
Stanford University, Stanford, California 94305

Crystal Structure and Pyrolysis of $[(Os(NH_3)_5)_2(\eta^2:\eta^2-\mu-C_6H_6)]^{4+}$: Evidence for the Formation of a Stable $\eta^2:\eta^6-\mu$-Arene Complex

W. Dean Harman, Matthew Gebhard, and Henry Taube*

Received April 25, 1989

In the course of investigating η^2-bound arene complexes of pentaammineosmium(II),[1] we have consistently observed the formation of trace amounts of a species in which the arene appears to act as a bridging ligand. Recently we reported that $[Os(NH_3)_5(\eta^2-C_6H_6)](OTf)_2$ ($OTf = CF_3SO_3^-$) (**1**), when allowed to stand in an inert solvent for 24 h, condenses to form the binuclear species $[(Os(NH_3)_5)_2(\eta^2:\eta^2-\mu-C_6H_6))](OTf)_4$ (**2**) and free benzene in high yield.[2] ^1H and ^{13}C NMR data indicate three inequivalent positions in the ring, and chemical shift data suggest that the metal centers engage separate double bonds. This bonding arrangement would result in a single *localized* olefin site that is expected to show enhanced reactivity relative to the free ligand. However, whereas single-metal coordination has been shown to activate an arene toward hydrogenation[3] or further coordination,[4] double-metal coordination appears to limit further reactivity: attempts to add a third pentaammineosmium(II) moiety were unsuccessful, as were our attempts to hydrogenate[3] or epoxidize[5] the complex. We attributed the failure of **2** to undergo these reactions to steric rather than electronic effects, reasoning that steric constraints require the metal centers to lie on opposite faces of the arene plane. To settle the question of geometry, we have determined the crystal structure for **2**.

Experimental Section

Compounds **1** and **2** were prepared according to procedures previously reported.[2] Crystals of **2** were grown from the vapor diffusion of ether into an acetone solution. A single crystal (approximately 0.4 mm^3) was sealed in a glass capillary tube along with a drop of mother liquor. The data set was acquired by using the $\theta-2\theta$ scan technique on a Syntex $P(2)_1$ diffractometer with graphite-monochromated Mo Kα radiation (Table I). The osmium positions were located for the space group $C2/c$ by Patterson techniques and the remaining atoms by difference Fourier synthesis. No attempt was made to locate or refine hydrogen atoms. Final full-matrix least-squares refinement was calculated with anisotropic temperature factors based on 5015 unique reflections over the range $6° < 2\theta < 55°$ with the condition $|F_o|^2 > 3\sigma|F_o|^2$. Over an irradiation period of 190 h, the intensity of standard reflections showed a decay of 4%. Both linear decay and empirical absorption corrections were applied. The observed and calculated structure factors and temperature factors are available as supplementary material.

The pyrolyses of **1** and **2** were carried out under vacuum (pressure > 1 μm) in a glass vessel immersed in an oil heat bath at temperatures ranging from 85 to 150 °C over periods of hours to days. The maximum yield of **4** (about 30%) was obtained by heating **2** for 16 h at 90 °C.

---

(1) Harman, W. D.; Sekine, M.; Taube, H. *J. Am. Chem. Soc.* **1988**, *110*, 5725.

(2) Harman, W. D.; Taube, H. *J. Am. Chem. Soc.* **1987**, *109*, 1883.

(3) Harman, W. D.; Taube, H. *J. Am. Chem. Soc.* **1988**, *110*, 7906.

(4) Harman, W. D.; Taube, H. *J. Am. Chem. Soc.* **1988**, *110*, 7555.

(5) The reaction of 1 with 1 equiv of *m*-chloroperbenzoic acid resulted in the slow oxidation of metal centers.